The Journal of the Astronautical Sciences (2019) 66:32–45
https://doi.org/10.1007/s40295-018-00147-y

Preliminary Results on Optimal Establishment of Solar Sail Formations

Khashayar Parsay[1] · **Hanspeter Schaub**[1]

Published online: 10 May 2019

Abstract

The solar sail formation establishment problem is solved for Earth-centered Sun-Synchronous orbits using optimal control theory, assuming that the deputy solar sail is capable of changing its attitude and that the chief solar sail flies in a Sun-synchronous orbit and does not employ active control. Because there is no analytic solution, numerical techniques are used to solve the optimal formation establishment problem. This paper demonstrates the existence of locally-optimal solutions to the solar sail formation establishment problem and provides a quantification of the solar sail's control effort.

Keywords Solar sail · Formation flying · Magnetosphere

Nomenclature

$\boldsymbol{a}_s$	Solar radiation pressure acceleration [km/s^2]
$\boldsymbol{\text{œ}}$	Array containing classical orbital elements $[a, e, \omega, M]^T$. a: semi-major axis [km], e: eccentricity, ω: argument of perigee [rad], M: mean anomaly [rad]
$\delta\boldsymbol{\text{œ}}$	Differential orbital elements of deputy with respect to chief
λ_s	Sun longitude measured from vernal equinox [rad]
k	Characteristic acceleration of solar sail [km/s^2]
$\mathcal{O}$	Local-vertical-local-horizontal (LVLH) frame
c	Denotes the chief solar sail

Electronic supplementary material The online version of this article (https://doi.org/10.1007/s40295-018-00147-y) contains supplementary material, which is available to authorized users.

✉ Khashayar Parsay
khashayar.parsay@colorado.edu

Hanspeter Schaub
hanspeter.schaub@colorado.edu

[1] University of Colorado (Boulder), Boulder, CO, USA

d	Denotes the deputy solar sail
R_E	Earth radius
SRP	Solar radiation pressure

Introduction

The ability of solar sails to create non-Keplerian orbits can significantly increase the science gain of certain space missions. Past and current magnetosphere missions employ conventional spacecraft formations for in situ observations of the geomagnetic tail. Conventional spacecraft flying in inertially fixed Keplerian orbits are only aligned with the geomagnetic tail once per year, since the geomagnetic tail is always aligned with the Earth-Sun line, and therefore, rotates annually. National Aeronautics and Space Administration's (NASA) Time History of Events and Macroscale Interactions during Substorms (THEMIS), Magnetospheric Multi-Scale (MMS), and Radiation Belt Storm Probes (RBSP) missions, along with European Space Agency's (ESA) Cluster II mission are some of the currently active magnetosphere missions that employ multiple spacecraft flying in Keplerian orbits to achieve their scientific objectives [1–3]. As illustrated in Fig. 1, solar sails are able to artificially create sun-synchronous orbits such that the orbit apse line remains aligned with the geomagnetic tail line throughout the entire year [4–6]. This continuous presence in the geomagnetic tail can significantly increase the science phase for magnetosphere missions.

McInnes and Macdonald propose a novel mission called GEOSAIL in which a solar sail is employed to create a Sun-synchronous orbit artificially [4]. GEOSAIL's initial feasibility study was carried out by ESA in 2007, but since then, there has been no update regarding mission funding and its future. Because studying the geomagnetic tail requires multiple spacecraft to fly in formation in order to separate spatial and temporal plasma variations, Mu et al. propose flying two solar sails in formation. Ref. [7, 8] propose flying two solar sails in a projected circular formation, which requires active control to maintain the formation due to the non-Keplerian nature of the proposed relative motion. Parsay and Schaub propose natural solar sail formations, which only requires maintaining a Sun-pointing attitude upon achieving the desired natural relative motion; the necessary conditions for a drift-free natural solar sail formation and the design of such formations for two-craft, triangle, and tetrahedron geometries are studied in Ref. [9–11].

This preliminary study aims to address the solar sail formation establishment problem for the most basic natural formation, namely the *string of pearl* formation, in Earth-centered Sun-synchronous orbits. It is assumed that the chief solar sail flies in a Sun-synchronous orbit, while the deputy solar sail adjusts its attitude to establish a desired string of pearl formation of a particular size. The main motivation is to seek the existence of solutions and quantify the control effort under the most ideal scenario. Therefore, only the in-plane dynamics is considered when solving the optimal control problem. Because each spacecraft is assumed to employ its own individual control without cooperating with other deputies, the presented problem formulation

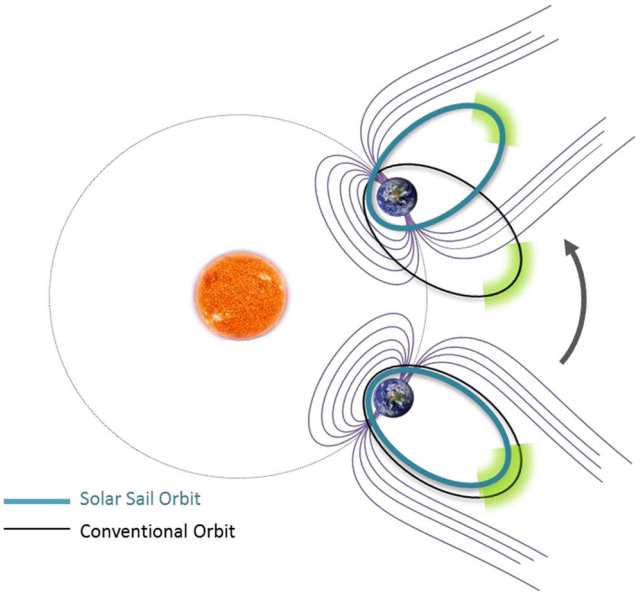

Fig. 1 Comparison of chemical and solar sail propulsion in geomagnetic tail exploration

may be expanded to include more deputies. This paper is organized as follows. The equations of motion for two solar sails flying in Sun-synchronous orbits is discussed in "Equations of Motion". The formulation of the optimal formation establishment problem is presented in "Problem Formulation for Optimal Formation Establishment". In "Numerical Solutions", the employed solution method and the numerical results are studied. Concluding remarks are given in "Conclusion".

Equations of Motion

For a flat, rigid, perfectly reflecting solar sail, the solar sail's acceleration due to the solar radiation pressure (SRP) is written as

$$\boldsymbol{a}_s = k\left(\hat{\boldsymbol{n}}_s \cdot \hat{\boldsymbol{n}}\right)^2 \hat{\boldsymbol{n}} \tag{1}$$

where $\hat{\boldsymbol{n}}$ is a unit vector normal to the sail surface, $\hat{\boldsymbol{n}}_s$ is a unit vector from the Sun to the Earth, and the parameter k is the sail's characteristic acceleration, which is defined as the acceleration experienced by the solar sail at a heliocentric distance of 1 astronomical unit (AU) while the sail's normal is directed along the sun-line [12].

As illustrated in Fig. 2, to create a Sun-synchronous orbit, a solar sail flying in the ecliptic plane employs a simple steering law consisting of the sail's normal vector continuously pointing along the Sun-line within the orbit plane such that the identities $\omega = \lambda_s$ and $\hat{\boldsymbol{n}} \cdot \hat{\boldsymbol{n}}_s = 1$ hold [4–6]. The required characteristic acceleration k to

precess the orbit Sun-synchronously is dependent on the shape of the orbit and is computed according to [4, 5]

$$k\left(a,e\right)=\frac{2}{3}\dot{\lambda}_s\frac{e}{\sqrt{1-e^2}}\sqrt{\frac{\mu}{a}} \tag{2}$$

In this problem formulation, the chief is assumed to fly in a Sun-synchronous orbit by maintaining a Sun-pointing attitude. Inspecting Fig. 2 and Eq. 1, the chief's SRP acceleration expressed in the chief's LVLH frame is,

$$^{\mathcal{O}_c}\boldsymbol{a}_{s_c}=\begin{bmatrix}a_{r_c}\\ a_{\theta_c}\end{bmatrix}^{\mathcal{O}_c}=k_c\begin{bmatrix}\cos\phi_c\\ \sin\phi_c\end{bmatrix}^{\mathcal{O}_c} \tag{3}$$

where the subscript c denotes the chief solar sail. It is assumed that the chief does not apply control to *cooperatively* achieve a desired relative motion; only the deputy is assumed to have the capability to change its attitude in order to establish a desired formation. The deputy solar sail is nominally maintaining a Sun-pointing attitude, but is capable of changing its orientation within the orbit plane by $\delta\phi$. The change in the deputy's orientation is assumed to have physical lower and upper limits. Therefore, the deputy's attitude varies from its nominal Sun-pointing attitude by $\delta\phi_{\min}\leqslant\delta\phi(t)\leqslant\delta\phi_{\max}$. The deputy's SRP acceleration expressed in the deputy's LVLH frame is written as,

$$^{\mathcal{O}_d}\boldsymbol{a}_{s_d}=\begin{bmatrix}a_{r_d}\\ a_{\theta_d}\end{bmatrix}^{\mathcal{O}_d}=k_d\begin{bmatrix}\cos\left(\phi_d+\delta\phi_d\right)\\ \sin\left(\phi_d+\delta\phi_d\right)\end{bmatrix}^{\mathcal{O}_d} \tag{4}$$

The two-body equations of motion for a spacecraft, governed by the Gauss' variation of parameters equations, are [13],

$$\dot{\mathfrak{oe}}=\boldsymbol{f}\left(\mathfrak{oe},\boldsymbol{u}\right)=\boldsymbol{A}+\boldsymbol{B}\left(\mathfrak{oe}\right)\boldsymbol{u} \tag{5}$$

where $\mathfrak{oe}=\begin{bmatrix}a & e & \omega & M\end{bmatrix}^T$ contains the classical orbital elements, $\boldsymbol{u}$ is the perturbing acceleration, and the matrices $\boldsymbol{A}$ and $\boldsymbol{B}\left(\mathfrak{oe}\right)$ are defined as,

$$\boldsymbol{A}=\begin{bmatrix}0 & 0 & 0 & n\end{bmatrix}^T \tag{6}$$

$$\boldsymbol{B}\left(\mathfrak{oe}\right)=\begin{bmatrix}\frac{2ea^2\sin f}{h} & \frac{2a^2p}{hr}\\ \frac{p\sin f}{h} & \frac{\left[(p+r)\cos f+re\right]}{h}\\ -\frac{p\cos f}{he} & \frac{(p+r)\sin f}{he}\\ \frac{b(p\cos f-2re)}{ahe} & -\frac{b(p+r)\sin f}{ahe}\end{bmatrix} \tag{7}$$

where f is true anomaly. Let $\overline{\mathfrak{oe}}$ denote the orbital elements of the formation comprising both the chief and deputy solar sails,

$$\overline{\mathfrak{oe}}=\begin{bmatrix}\mathfrak{oe}_c & \mathfrak{oe}_d\end{bmatrix}^T=\begin{bmatrix}a_c & e_c & \omega_c & M_c & a_d & e_d & \omega_d & M_d\end{bmatrix}^T \tag{8}$$

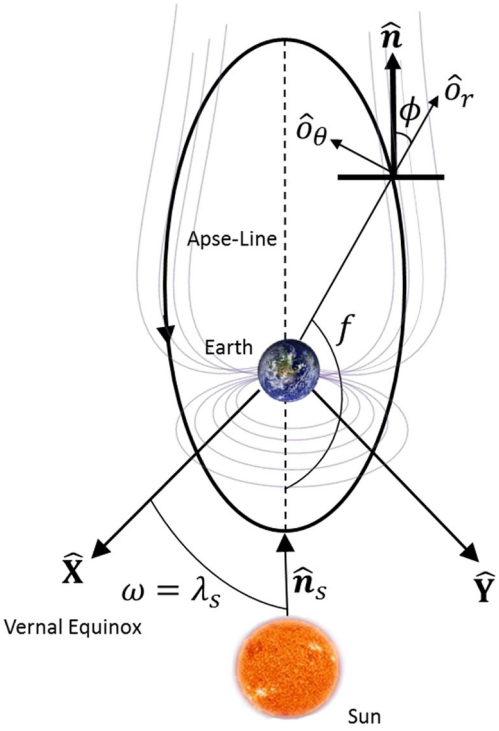

Fig. 2 Solar sail geometry in Sun-synchronous orbit

The equations of motion for the formation is written as,

$$\dot{\overline{\mathfrak{oe}}} = \overline{f}\,(\overline{\mathfrak{oe}}, \overline{a}_s) \tag{9}$$

where $\overline{a}_s$ includes the perturbing SRP accelerations for both the chief and the deputy solar sail.

The variations of the chief orbital elements under the SRP influence of Eq. 3 are illustrated in Fig. 3 for approximately 33 days for a 11 $R_E \times$ 30 R_E reference orbit that lies in the ecliptic. Both the semi-major axis and eccentricity experience periodic variations, but their net change over a span of an orbit is zero. Because the sail is maintaining a Sun-pointing attitude and the orbit lies within the ecliptic plane, there is no out-of-plane variations, as evident by Fig. 3c and d. Figure 3e shows the argument of perigee increasing by approximately one degree per day. This is a direct result of imposing the Sun-synchronous condition in Eq. 2. The sail size required to precess this reference orbit is 47 $\times$ 47 m^2, assuming that the sail weighs 160 kg and has an efficiency of 95%. The required sail size reduces to 41 $\times$ 41 m^2 if the sail's mass is 120 kg. NASA's Sunjammer mission, which was canceled in October 2014 prior to launch, planned to fly a 38 $\times$ 38 m^2 solar sail with a total mass of 32 kg [14]. Thus, the assumptions made in this paper about the sails' size and mass fall within the realm of current or near future technology.

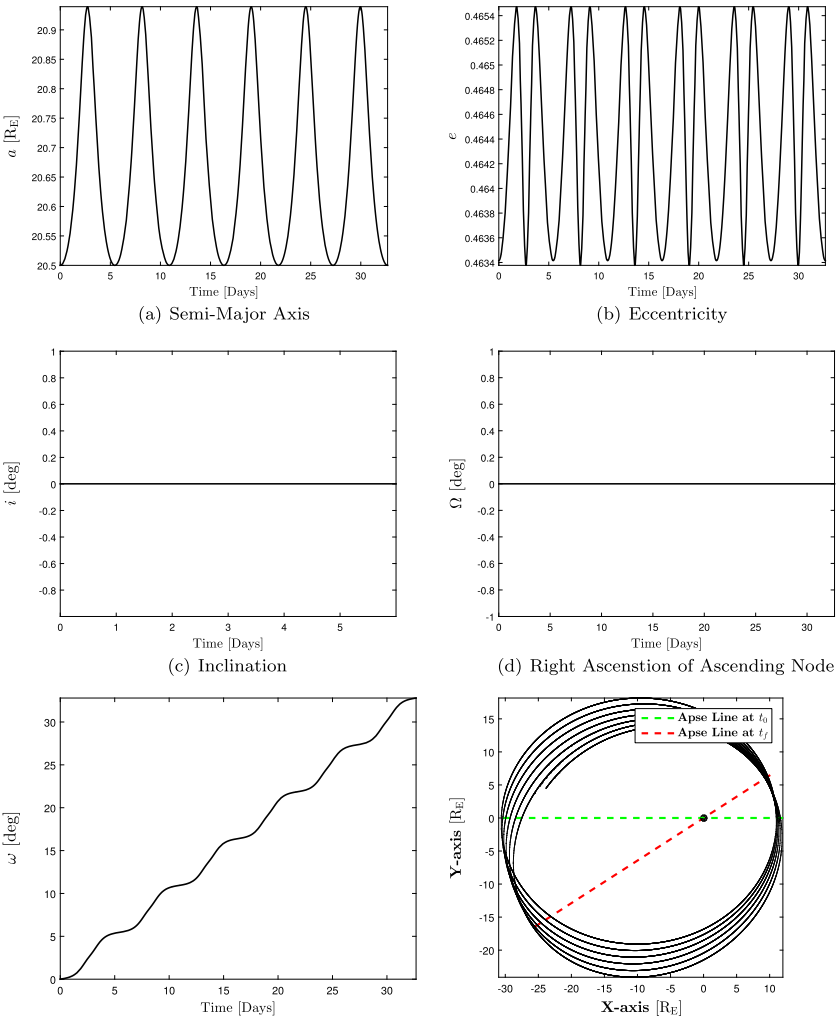

Fig. 3 Sail's orbital elements variations

Problem Formulation for Optimal Formation Establishment

The formation establishment problem is formulated as follows,

$$\begin{aligned}
&\text{minimize} && J = \int_{t_0}^{t_f} \delta\phi_d^2(t)\ \mathrm{d}t \\
&\text{with respect to} && \dot{\overline{\boldsymbol{\alpha}}} = \overline{\boldsymbol{f}}\left(\overline{\boldsymbol{\alpha}}, \overline{\boldsymbol{a}}_s\right) \\
&\text{subject to} && \overline{\boldsymbol{\alpha}}\left(t_0\right) = \overline{\boldsymbol{\alpha}}_0 \\
& && \delta\boldsymbol{\alpha}\left(t_f\right) = \delta\boldsymbol{\alpha}_f \\
& && \delta\phi(t_0) = \delta\phi(t_f) = 0 \\
& && \delta\phi_{\min} \leqslant \delta\phi(t) \leqslant \delta\phi_{\max}
\end{aligned} \tag{10}$$

where the differential orbital elements $\delta\mathbf{oe}$ are defined as,

$$\delta\mathbf{oe}(t) = \mathbf{oe}_d(t) - \mathbf{oe}_c(t) = \left[\begin{array}{cccc} \delta a & \delta e & \delta\omega & \delta M \end{array}\right]^T \tag{11}$$

The array $\delta\mathbf{oe}_f$ contains the desired osculating differential elements at the final boundary epoch. The most simple form of a natural formation is the leader-follower or the string of pearls formation. This formation requires both the chief and deputy to be in the same orbit and consequently have the same characteristic acceleration based on Eq. 2. The same characteristic acceleration implies that the two solar sails must have the same design and reflective surface area. Building two identical solar sails may reduce cost and complexity in terms of design. For a natural leader-follower formation, the desired osculating orbital elements at the final epoch are,

$$\delta\mathbf{oe}_f = \left[\begin{array}{cccc} \delta a_f & \delta e_f & \delta\omega_f & \delta M_f \end{array}\right]^T = \left[\begin{array}{cccc} 0 & 0 & 0 & \delta M_f \end{array}\right]^T \tag{12}$$

Depending on the value of δM_f, the leader-follower formation has a different size. Thus, δM_f directly controls the formation size, which is typically dictated by the scientists for magnetosphere missions. It is assumed that both the chief and deputy start with a Sun-pointing attitude flying in a Sun-synchronous orbit. Because the desired relative motions are natural, the deputy solar sail must have a Sun-pointing attitude once the formation is established, otherwise the relative secular drift rates due to the relative SRP forces will lead to the degradation of the achieved formation. For these reasons, the constraint $\delta\phi(t_0) = \delta\phi(t_f) = 0$ is included in the formation establishment problem in Eq. 10, which assures that the deputy starts and ends with a Sun-pointing attitude.

For this formation establishment problem, two different time horizons are examined. At first, it is assumed that the deputy solar sail achieves the desired relative motion within 0.5 orbit (denoted by T-1), as illustrated in Fig. 4a. The same problem is then solved assuming that the formation is established in 1.5 orbits (T-2), as shown in Fig. 4b.

Similarly, two initial boundaries ($\overline{\mathbf{oe}}_0$) are selected to further investigate the sensitivity of the control effort to initial relative geometry. The first initial boundary (IB-1) is assumed to be the post-deployment state followed by 3 coasting orbits. The second initial boundary (IB-2) is assumed to be the post-deployment state without any coasting phase.

The deployment scenario considered is as follows. The two sails are released sequentially at the perigee of the operational mission orbit. The chief is released along the local velocity direction. The deputy sail is released in a slightly different direction than the velocity to avoid close approaches. In this study, the deputy is assumed to be released along a direction that is 1° off the local velocity direction while lying within the orbit plane. The chief sail is released first, followed by the deputy after a buffer time to further reduce the chance of a close approach immediately after the deployment. During the next 3 orbits, the sails deploy their reflective surface and achieve the desired Sun-pointing mission attitude. The 3 orbit coasting time allows the ground segment to perform orbit and attitude determination before establishing the desired formation. The corresponding differential orbital elements immediately

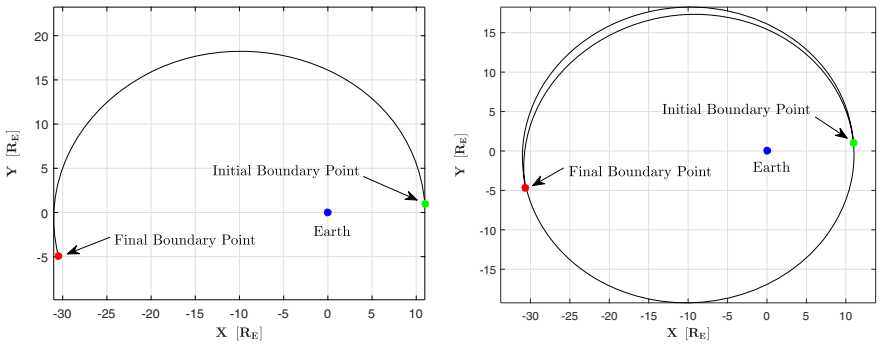

(a) 0.5 Orbit (b) 1.5 Orbit

Fig. 4 Time-horizons used in solving the optimal formation establishment problem

after deployment are summarized in Table 1. More details on this simple deployment strategy can be found in Ref. [15].

Numerical Solutions

Solution Method

A fast direct method to solve optimal control problems is the *Legendre Pseudo-Spectral Method*. This method uses Legendre polynomials to approximate (discretize) states and controls for each segment between nodes. The nodes are selected using a Gaussian quadrature method. Once the problem is discretized, a nonlinear programming (NLP) solver is used to solve for the states and the required control. A version of this method is implemented in the software package DIDO [16]. Many direct methods do not produce costate information, which may be considered a drawback because it inhibits the verification of optimality. The main advantage of DIDO is that it is capable of computing accurate values for the adjoint functions without solving the associated necessary conditions. This allows for the checking of the optimality conditions once DIDO converges on an optimal solution.

Once the optimal control problem is solved, the solution is first evaluated for its feasibility. This is to assure that the solution satisfies the the ordinary differential equations (ODE), since there is no propagation involved in the Legendre Pseudo-Spectral method employed to solve the optimal control problem. Once a solution

Table 1 Post-deployment differential elements

Differential Element	Value	Unit
δa	-0.7	km
δe	-4.24×10^{-6}	–
$\delta\omega$	$+0.021$	deg

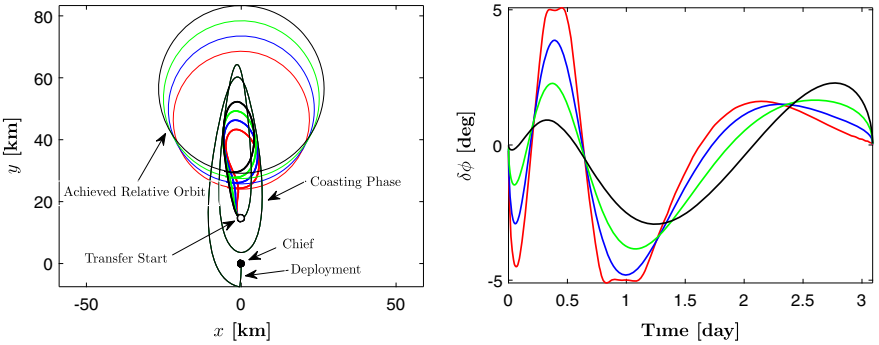

(a) Relative Trajectory in Chief's LVLH Frame (radial vs. along-track plane)

(b) Control Effort

Fig. 5 Leader-follower formation establishment (IB-1 — T-1)

satisfies the ODE feasibility test, the necessary conditions are numerically checked to test the optimality of the solution.

Results

The optimal formation establishment problem is solved using the initial boundary IB-1 and the time horizon T-1 for four different formation sizes as shown in Fig. 5. The entire formation deployment and establishment scenario as seen by the chief solar sail is illustrated in Fig. 5a. As noted earlier, the chief sail is released first along the velocity direction. After 25 minutes of buffer time, the deputy sail is released along a direction that is 1° off the local velocity direction. Because there is a difference between the orbit periods of the two sails due to nonzero δa, the deputy experiences a secular drift in the along-track direction during the next 3 orbits. After the coasting time, the deputy begins changing its attitude to achieve the leader-follower formation at the chief's orbit apogee.

The controller's effort is shown in Fig. 5b. In all cases, the control effort falls within the specified imposed constraints, which are taken to be $\pm 6°$. For the initial boundary IB-1, the most optimal formation is achieved for the $\delta M_f = +0.0205°$ case, which leads to the smallest cost of $J = 0.00025$ as evident by Table 2 and Fig. 5b. Although the required attitude change does not exceed the limits defined, the rate of change of $\delta\phi$ is relatively high for the two cases shown in blue and red. Given

Table 2 Cost vs. formation size in leader-follower formation establishment

Trajectory	Desired δM_f	IB-1 T-1 Case	IB-2 T-1 Case
Red	$\delta M_f = +0.0169°$	$J = 0.00072$	$J = 0.00034$
Blue	$\delta M_f = +0.0181°$	$J = 0.00047$	$J = 0.00051$
Green	$\delta M_f = +0.0193°$	$J = 0.00031$	$J = 0.00075$
Black	$\delta M_f = +0.0205°$	$J = 0.00025$	$J = 0.00110$

the size of the solar sail assumed in this study, such angle rates may or may not be achievable. Thus, picking the right formation size for a given initial boundary is important.

The time history of the adjoint variables are used to check the necessary conditions on the optimality of the feasible solutions. For instance, the well-known *gradient normality condition* [16–18] requires that,

$$\frac{\partial \bar{\mathcal{H}}}{\partial \boldsymbol{u}}(\boldsymbol{\lambda}^*(t), \boldsymbol{x}^*(t), \boldsymbol{u}^*(t), t) = \frac{\partial \bar{\mathcal{H}}}{\partial \delta\phi}(\boldsymbol{\lambda}_d^*(t), \overline{\boldsymbol{\alpha}}_d^*(t), \delta\phi^*(t), t) = 0 \tag{13}$$

As shown in Fig. 6, for one of the converged solutions, the gradient normality condition is satisfied to an acceptable numerical precision. The variations in the differential elements throughout the formation establishment process is illustrated in Fig. 7. It is evident that the initial differential orbital elements in Table 1 are nullified as desired to establish the leader-follower formation. Note that the differential element δa increases in magnitude from -0.7 km at the initial boundary to -26 km before it is nullified at the final epoch. Similarly, there is a significant variation in the δe before the formation is established.

To illustrate the effects of the initial boundary (initial relative geometry of the two sails) on control performance, the optimal formation establishment is solved for the same desired formation, assuming the initial boundary condition IB-2. The relative trajectory and the deputy's control effort are illustrated in Fig. 8. The corresponding cost to each of the desired relative geometries are shown in Table 2. For this initial boundary, the most optimal control effort corresponds to the smallest desired relative motion of $\delta M_f = +0.0169°$. As the formation size increases, the required control becomes less optimal. For the case of $\delta M_f = +0.0205°$, the rate of change of $\delta\phi_d$ is high, which may or may not be achievable for the deputy solar sail. Comparing Fig. 8 to Fig. 5, it is evident that a different initial relative geometry yields a *significantly* different optimal control for the same desired formation. Therefore, a careful formation deployment strategy must be selected, since the deployment directly affects the relative initial geometry between the two sails before the formation is established. This is typically not an issue for spacecraft that use chemical

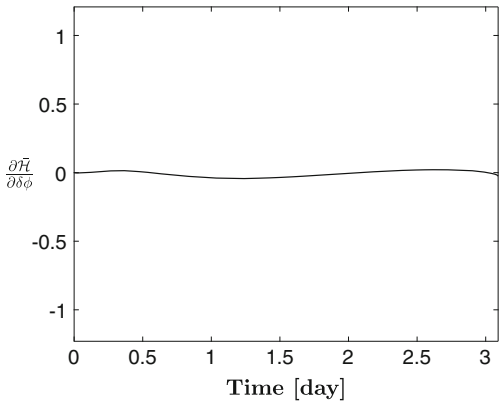

Fig. 6 Checking first-order optimality conditions

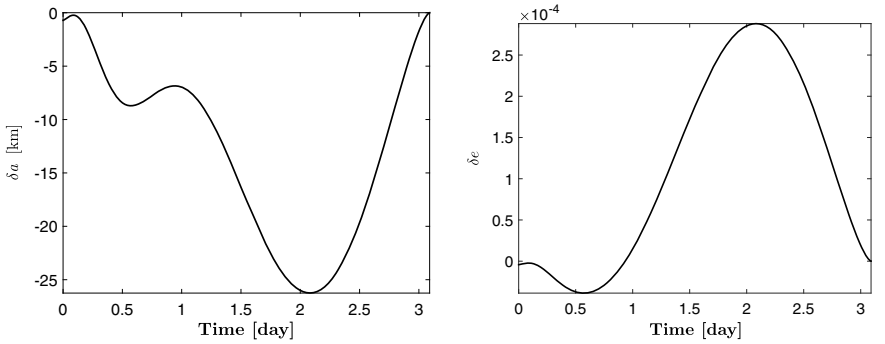

(a) Difference in Semi-Major Axis (b) Difference in Eccentricity

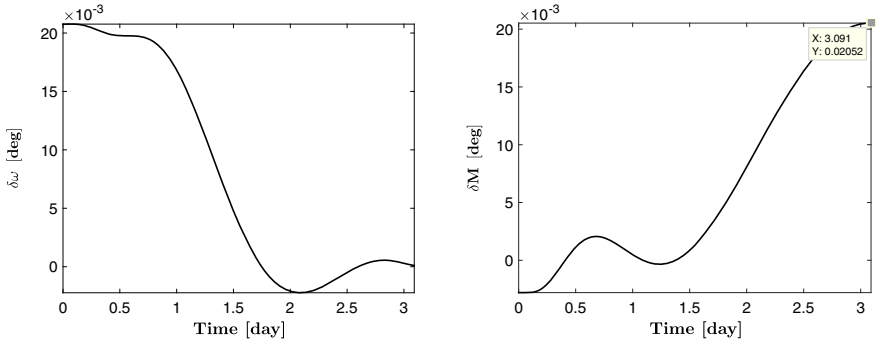

(c) Difference in Argument of Perigee (d) Difference in Mean Anomaly

Fig. 7 Variation in differential elements throughput the formation establishment

propulsion. However, in the case of solar sails and systems lacking high thrust propulsion, the deployment strategy may be used as a knob to turn for setting up the initial relative geometry, such that the sail's effort to achieve the desired relative motion is minimized.

To illustrate the effect of the time horizon on the control, the formation establishment problem is solved using the IB-1 boundary conditions and the time span

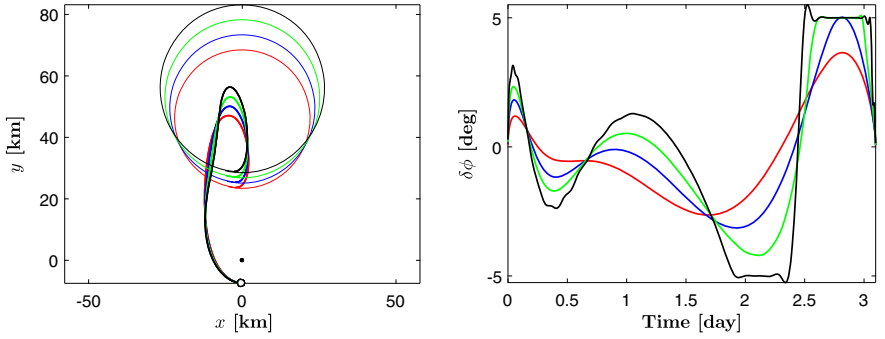

(a) Relative Trajectory in Chief's LVLH Frame (radial vs. along-track plane) (b) Control Effort

Fig. 8 Leader-follower formation establishment (IB-2 — T-1)

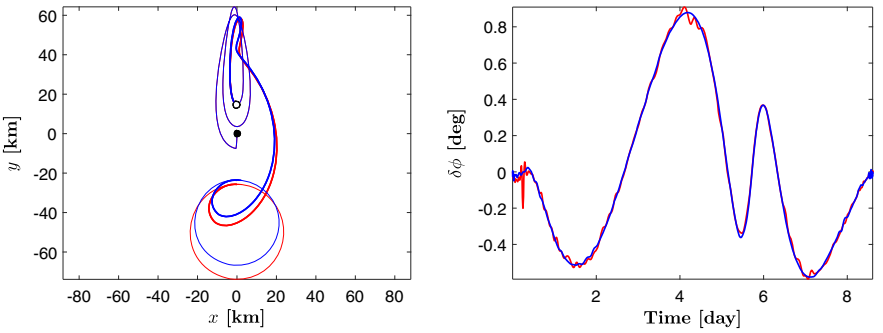

(a) Relative Trajectory in Chief's LVLH Frame (radial vs. along-track plane)

(b) Control Effort

Fig. 9 Leader-follower formation establishment (IB-1 — T-2)

T-2. Two trajectories are generated for two different formation sizes as illustrated in Fig. 9. The increase in the time horizon directly increases the computational time for the numerical optimal control solver, which may be an issue in practice.

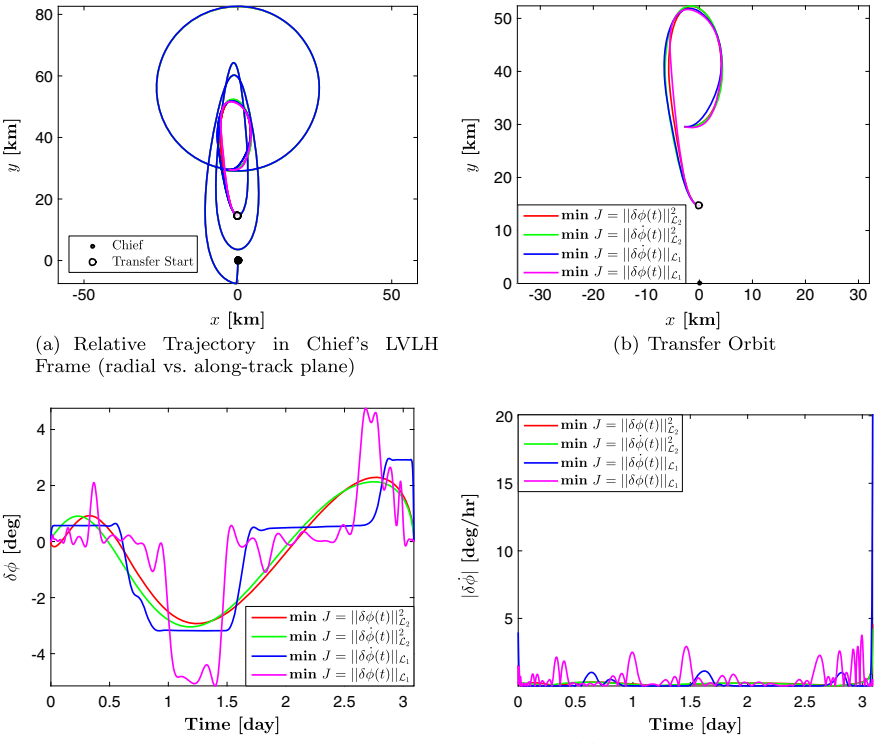

(a) Relative Trajectory in Chief's LVLH Frame (radial vs. along-track plane)

(b) Transfer Orbit

(c) Changes in Attitude

(d) Changes in Angle Rate

Fig. 10 The effects of employing different cost functions for a specific desired formation

Effects of Changing the Measure of Optimality

As evident from Eq. 10, the cost function selected is the $\mathcal{L}_2$ norm of the change in the deputy's orientation, which leads to smooth changes in $\delta\phi$. The effects of changing the measure of optimality is illustrated in Fig. 10 for four different cost functions, namely, $||\delta\phi(t)||^2_{\mathcal{L}_2}$, $||\delta\dot{\phi}(t)||^2_{\mathcal{L}_2}$, $||\delta\dot{\phi}(t)||_{\mathcal{L}_1}$, and $||\delta\phi(t)||_{\mathcal{L}_1}$. As evident from Fig. 10a and b, the desired leader-follower formation is established in all cases. The main challenge in controlling a solar sail's attitude are the physical limits on the angular velocity that a large solar sail is able to achieve. For this reason, it is crucial to assure that the sail's orientation is not subjected to rapid changes. To achieve slow changes in orientation, the cost function is changed from minimizing the angle $\delta\phi$ to minimizing the angle rate $\delta\dot{\phi}$. It is evident in Fig. 10c and d that minimizing the $\mathcal{L}_1$ norm of $\delta\dot{\phi}$ leads to nearly zero rates throughout the maneuver but requires rapid changes in attitude at the boundary points, which may or may not be achievable depending on the type of attitude control system on-board. Due to the high frequency of variations in the deputy's attitude, which is difficult to achieve for a solar sail, it is concluded that the $\mathcal{L}_1$ norm cost function does not yield solutions that are practical.

Conclusion

In this paper, the problem of establishing a leader-follower solar sail formation is discussed. First, a deployment scenario into the mission orbit is considered. From this deployment scenario, the relative geometry between the two solar sails are estimated after they are injected into the mission orbit. This is a crucial step before employing active control to achieve a desired formation; it allows for a solution to the formation establishment problem, assuming a pragmatic initial relative geometry.

The formation establishment problem is solved using optimal control theory, assuming that the deputy solar sail is capable of changing its attitude and that the chief solar sail flies in a Sun-synchronous orbit and does not employ active control. Because there is no analytic solution, numerical techniques are used to solve the optimal formation establishment problem. Solutions to the optimal control problem are found for a leader-follower formation of various sizes. It is shown that changing the formation size may require a significantly different control effort for the same initial boundary conditions. The effects of changing the initial relative geometry for achieving the same desired relative motion is subsequently explored and it is shown that small changes to relative initial geometry can have a significant impact on the control effort required to achieve the same desired relative motion. The effects of changing the measure of optimality is also investigated. It is demonstrated that smooth quadratic cost functions ($\mathcal{L}_2$ norms) lead to smoother control efforts when compared to non-smooth cost functions ($\mathcal{L}_1$ norms). This is especially important for solar sails since they are not capable of making abrupt changes to their orientations.

This paper only considered in-plane variations in the sail's attitude for establishing a desired relative geometry. Both in-plane and out-of-plane changes in a sail's orientation will be necessary in practice for establishing a desired relative motion,

even if the sails lie in the same plane initially. The relative third-body effects will certainly create small relative out-of-plane separations that the deputy solar sails must correct for before establishing the desired in-plane leader-follower formation. While the rigid flat-plate SRP model may be sufficient for preliminary orbit analysis, an accurate SRP model that is validated by historical data is needed to develop a practical simulation tool. Moreover, because of the highly coupled orbit-attitude dynamics of solar sails, anything but a six DoF simulation is susceptible to inaccuracies that may not be negligible when flying two large solar sails in close proximity of each other.

References

1. Angelopoulos, V.: The THEMIS mission, the THEMIS mission, pp. 5–34. Springer, New York (2009)
2. Angelopoulos, V.: The ARTEMIS mission, the ARTEMIS mission, pp. 3–25. Springer, New York (2010)
3. Escoubet, C., Schmidt, R., Goldstein, M.: Cluster-science and mission overview, the Cluster and Phoenix missions, pp. 11–32. Springer, Dordrecht (1997)
4. McInnes, C.R., MacDonald, M., Angelopolous, V., Alexander, D.: Geosail: exploring the geomagnetic tail using a small solar sail. J. Spacecr. Rocket. **38**(4), 622–629 (2001)
5. Macdonald, M., Hughes, G., McInnes, C., Lyngvi, A., Falkner, P., Atzei, A.: Geosail: an elegant solar sail demonstration mission. J. Spacecr. Rocket. **44**(4), 784–796 (2007)
6. Macdonald, M., McInnes, C.: Analytical control laws for planet-centered solar sailing. J. Guid. Control Dynam. **28**(5), 1038–1048 (2005)
7. Mu, J., Gong, S., Li, J.: Reflectivity-controlled solar sail formation flying for magnetosphere mission. Aerosp. Sci. Technol. **30**(1), 339–348 (2013)
8. Mu, J., Gong, S., Li, J.: Coupled control of reflectivity modulated solar sail for GeoSail formation flying. J. Guid. Control Dynam. **38**(4), 1–12 (2014)
9. Parsay, K.: Invariant Solar Sail Formations in Elliptical Sun-Synchronous Orbits. PhD thesis, University of Colorado (Boulder) (2016)
10. Parsay, K., Schaub, H.: Drift-free solar sail formations in elliptical Sun-synchronous orbits. Acta Astronaut. **139**, 201–212 (2017)
11. Parsay, K., Schaub, H., Schiff, C., Williams, T.: Improving magnetosphere in situ observations using solar sails. Adv. Space Res. **61**, 74–88 (2017)
12. McInnes, C.R.: Solar sailing: technology, dynamics and mission applications. Springer, London (2004)
13. Battin, R.H.: An introduction to the mathematics and methods of Astrodynamics. AIAA education series, revised ed. (1999)
14. Barnes, N.C., Derbes, W.C., Player, C.J., Diedrich, B.L.: Sunjammer: a solar sail demonstration, Advances in Solar Sailing, pp. 115–126. Springer, Berlin (2014)
15. Parsay, K., Schaub, H.: Establishment of natural solar sail formation using solar electric propulsion. J. Guid. Control Dynam. **39**(6), 1417–1425 (2015)
16. Ross, I.M.: A primer on pontryagin's principle in optimal control. Collegiate Publishers (2015)
17. Kirk, D.E.: Optimal control theory: an introduction. Courier Corporation, Chelmsford (2012)
18. Longuski, J.M., Guzmán, J.J., Prussing, J.E.: Optimal control with aerospace applications, vol. 32. Springer Science & Business Media, New York (2013)